Ain Shams Engineering Journal (2015) 6, 17–24

Ain Shams University

Ain Shams Engineering Journal

www.elsevier.com/locate/asej
www.sciencedirect.com

CIVIL ENGINEERING

Locating the site of diagonal tension crack initiation and path in reinforced concrete beams

H.S.S. Abou El-Mal *,[1], A.S. Sherbini [2], H.E.M. Sallam [3]

Civil Engineering Dept., Jazan Univ., Jazan 706, Saudi Arabia

Received 21 October 2013; revised 14 February 2014; accepted 14 October 2014
Available online 22 November 2014

KEYWORDS

RC beams;
Fiber reinforced concrete;
Diagonal tension crack;
Shear failure

Abstract The most favorable site of diagonal tension crack initiation has been attempted to be located. Due to the numerous interacted parameters affecting both site and angle of diagonal tension crack initiation, twelve possible sites were investigated, at midheight of the shear span and at the bottom surface near the support of the beam with vertical and diagonal orientations. The first diagonal tension crack initiated from the bottom tip of the diagonal pre-crack at midheight of the beam as a result of constraint release. To verify the previous finding, a single diagonal pre-crack has been created at midheight of only one side of the shear spans in both normal and fiber reinforced concrete (FRC) beams. FRC beam showed different behavior, where couple of diagonal tension cracks initiated at both sides from the tip of flexural cracks regardless of the existence of pre-crack at one side of the beam.

1. Introduction

Even though the shear behavior of reinforced concrete has been studied for more than a century, the problem of determining the shear strength of reinforced concrete beams remains open to discussion. The shear strengths predicted by different current design codes [1–5] for a particular beam section can vary by more than the double. In contrast, the flexural strengths predicted by the same codes are unlikely to vary by more than 10%. For flexure, the plane sections hypothesis forms the basis of a universally accepted, simple, rational theory for predicting flexural strength. In addition, simple experiments can be performed on reinforced concrete beams subjected to pure flexure and the clear results from such tests have been used to improve the theory. In shear, there is no agreed basis for a rational theory, and experiments cannot be conducted on reinforced concrete beams subjected to pure shear [6]. Shear strength is still a controversial subject,

* Corresponding author at: Department of Civil Engineering, Faculty of Engineering, Jazan University, 4425-Arrawabi, Unit #2, Jazan 82822-6694, P.O. Box 706, Saudi Arabia. Tel.: +966 173217135, cell: +966 536359723; fax: +966 173310463.
E-mail address: heshnan@yahoo.com (H.S.S. Abou El-Mal).
[1] On sabbatical leave from Civil Engineering Department, Menofia University, Shibin El-Kom, Egypt.
[2] On sabbatical leave from Civil Engineering Department, Suez Canal University, Ismailia, Egypt.
[3] On sabbatical leave from Materials Engineering Dept., Zagazig Univ., Zagazig 44519, Egypt.

Peer review under responsibility of Ain Shams University.

Production and hosting by Elsevier

http://dx.doi.org/10.1016/j.asej.2014.10.006

specially when dealing with concrete. The main difficulty is that, concrete is a composite, non-homogeneous, and non-isotropic material that cracks at a low tension stress. Moreover, the shear-span-to-depth (a/d) ratio of a beam affects the load path, which in turn, has a significant influence on the beam shear capacity [7].

One of the most accepted traditional shear tests on a reinforced concrete beam is 4 PB. The region of the beam between the two point loads is subjected to pure flexure, whereas the shear spans of the beam are subjected to constant shear and linearly varying moment. Because the behavior of this member is changing from section to section along the shear span, it is difficult to use the results of such a test to develop a general theory for shear behavior. Thus, if a relationship is sought between the magnitude of the shear force and the developed strains in stirrups, it will be found that the strain magnitude is different for every stirrup and is also different over the height of each stirrup. Generally, the shear failure of a reinforced concrete beam is directly related to the diagonal tensile cracking that develops in the direction perpendicular to the principal tensile stress axis [6].

The shear behavior of concrete beams depends on the development of the two shear load transfer mechanisms namely: arch action and beam action. In brief, a load transferred in arch action goes directly from the loading point to the support while a load transferred in beam action goes through a truss before reaching to the support. The extent of arch and beam action depends highly on the shear-span-to-depth a/d ratio. Beam action is the dominant load transfer mechanism in slender and very slender beams (a/d ratios are between 2.5 and 6 or greater), while arch action develops in short and very short beams (a/d ratios are between 1 and 2.5 or smaller). For slender beams with no or a low level of web reinforcement, the typical failure mode is diagonal-tension failure. This type of failure is sudden and is due to the loss of equilibrium after the development of inclined flexure–shear cracks. If more web reinforcement is provided in slender beams, the mode of failure changes to shear–compression failure, which is a failure due to concrete crushing above the tip of a shear crack. Short beams fail in shear–compression failure, but they also commonly fail in shear–tension failure, which is bond failure due to secondary shear cracking along the tensile reinforcement. For very short beams, arch action dominates the shear transfer mechanism resulting in a near-uniform tensile force along the longitudinal tensile steel, which often leads to anchorage failure at the support. If adequate anchorage is provided for very short beams, web crushing failure is likely to occur [8]. To provide an accurate and consistent shear prediction for beams, a valley of diagonal tension failure could be achieved by adopting Kani Valley theory. The effect of tensile reinforcement of the beams, the relative flexural to ultimate moment of the beam M_u/M_{fl}, and the variation of shear-span-to-depth (a/d) ratio are considered [9,10].

2. Objective

The objective of the current work was to locate the most favorable site and path of diagonal tension crack initiation in both normal and fiber reinforced concrete beams. A parametric study concerning the inherent constraints surrounding the initiated crack was conducted to achieve that objective.

3. Experimental programme

The experimental study to accomplish the objective of this work was divided into three groups, pilot beam, virgin beams, and one sided precracked beams. All tested RC beams were large scale of $152 \times 254 \times 2000$ mm in dimension.

All groups were examined under four point bending, and designed to fail within shear span under the generated diagonal tension cracks (DT failure). Deficient shear reinforcement accompanied with well designed flexural reinforcement guaranteed such shear failure mechanism. Adopting Kani Valley theory a/d for current work was kept equal to 2.814. The critical $(a/d)_c$ for such configuration to force DT cracks equals (2.39), as will be detailed.

The concrete used in this test programme is high strength, self compacting, ready mix concrete (HSSCRMC) supplied from HOGG ready mix plant, Waterloo, Canada. The compressive strength of the concrete was 74 MPa and its tensile strength was 8 MPa. Steel fibers (hooked end RL-45/50-BN DRAMIX steel fiber) with mechanical properties shown in Table 1 were added on site at the conveying truck mixer when needed for fiber reinforced concrete beams fabrication.

Reinforcement steel with yield strength of 400 MPa caging was designed to achieve high flexural strength (bottom reinforcement 3 Dia 16), and deficient shear reinforcement (stirrups 2.5 Dia 8/m). The steel reinforcement was instrumented using three strain gages on the bottom reinforcement and one strain gage on each stirrup prior to concrete casting as shown in Fig. 1 .A full protocol of preparing reinforcement bars Prior to installing the strain gages was carried out. The strain gages were attached to the bars using special cement recommended by the manufacturer. The strain gages and the connecting terminals were covered with wax to protect the gages from damage during the concrete casting as shown in Fig. 1. Another group of strain gages was attached to the concrete surface at different positions. All beams were tested using a computer controlled actuator with a capacity of 440 kN and a data acquisition system recording the readings of load cell, strain gages, and LVDTs as shown in Fig. 2.

Table 1 DRAMIX data sheet.

Geometry	Length (L) 45/50.0 mm	Performance Class: 45	Aspect ratio L/d = 48	Diameter 1.05 mm
Specifications	Tensile strength 1000 N/mm^2	Coating None	Carbon content Low carbon	#/kg 2800 fibers/kg

DRAMIX **RL-45/50-BN** ($R_{ound} - L_{oose}$ class 45–50 mm $B_{right\text{-}low\ carbo}N$)

Figure 1 Strain gauges fitting on stirrups and tension reinforcement.

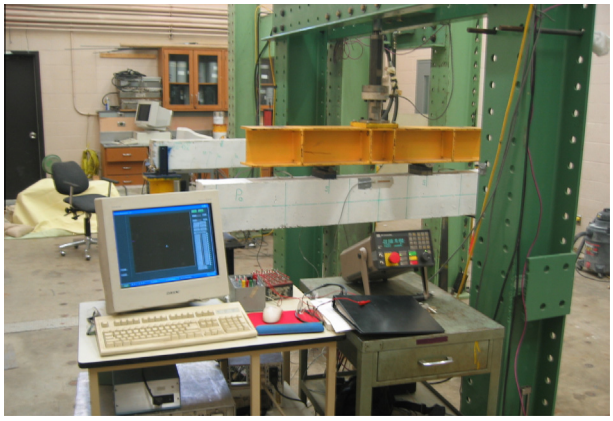

Figure 2 Four point bending test setup.

The whole work took place in two stages. In the first stage, one pilot beam with plain concrete matrix (PC.) was cast and tested, then in the second stage two groups of beams were fabricated. A couple of virgin RC beams of both steel fiber reinforced concrete matrix SFRC and plain concrete matrix PC with no cracks were cast and tested under the same configuration to work as a control group. Another couple of RC beams of both types of concrete with one sided 5.0 cm long crack along the favorable site and orientation determined from the pilot beam were cast and tested under the same configuration to assure the pilot beam findings.

4. Stage one, the pilot beam

Four groups of pre-cracks, each of three cracks was installed to the beam using 5.0 cm wide strips of natural rubber latex membrane of (0.02 in.) 0.5 mm thickness to create the pre-cracked positions as shown in Fig. 3. Each group was set in a different position with different orientation regarding arch action and beam action of the stress distribution as shown in Fig. 4 to investigate the favorable shear crack position and direction.

5. Preparation of beam details

To evaluate the influence of shear span on the shear–moment interaction phenomenon adopting Kani Valley theory, the area As of the longitudinal reinforcement was designed to obtain a premature shear mode of failure forcing diagonal tension

Figure 3 Manufacturing pilot beam with pre-cracks groups.

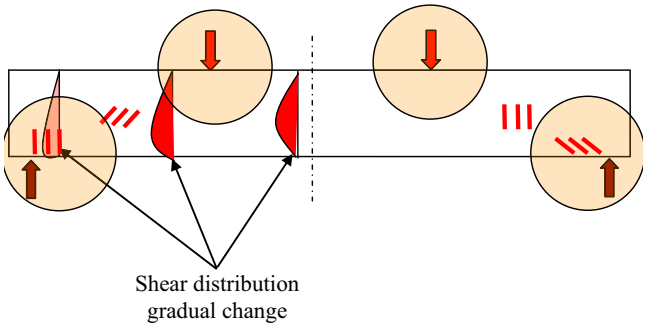

Figure 4 Proposed positions and orientations of pre-cracks.

failure to dominate. The ultimate moment of the beam, in the presence of shear, evaluated as the sum of the two contributions due to beam and arch effects, is provided by the following expression [7]:

$$Mu = [(0.83\xi\rho^{1/3}fc^{1/2}(a/d)) + (206.9\xi\rho^{5/6}(a/d)^{-3/2})]bd^2$$

where:

(ρ) is the tensile reinforcement ratio evaluated with reference to the effective beam depth d, (ρ) = As/(bd).

(fc) is the compressive concrete strength in MPa.

(a/d) is the shear span-to-depth ratio.

(ξ) is a function taking into account the aggregate size effect.

$\xi = 1/\sqrt{(1 + d/(25da))}$

(d) is the effective beam depth d = Height (h) – cover-bar diameter/2.

(da) is the maximum size of the aggregate.

The flexural capacity of the beam, calculated according to ACI Building Code recommendations [1], is expressed as

$$M_{fl} = bd^2\rho f_y(1 - \rho f_y/1.7fc)$$

where f_y is the yield strength of the reinforcing bars.

All values of Parameters in The Current Study are tabulated in Table 2.

The relative flexural capacity Mu/M_{fl} with variation in the dimensionless shear span to depth ratio proves to be that shown in Fig. 5, and the data necessary to construct the valley of diagonal failure [9] are given in Table 2. In particular, fc is obtained as the mean value of the cylindrical strength of three specimens of plain concrete; f_y is the mean value obtained by the tensile test on three specimens of steel bar. The Mu/M_{fl} versus a/d schematic drawing shows a minimum value corresponding to $(a/d)_c \approx 2.39$, and this value of the a/d ratio is a "critical value" because it discriminates between two failure modes. For $a/d > (a/d)_c$ the beam mechanism governs and the failure is usually termed as a diagonal-tension (DT) failure. While for $a/d < (a/d)_c$ the arch mechanism governs and the failure is usually termed as a shear-compression (SC) failure. For stirrups installation, two longitudinal bars with diameter 13 mm were inserted in the compressive region of the beam, in order to assure a good arrangement of the stirrups and enhance the compressive capacity of section above the neutral axis.

Table 2 Values of parameters in the current study.

ρ = As/bd	0.017
fc in MPa	74.0 MPa
d	254-15-8 = 231
a/d	650/231 = 2.814
ξ	0.721
da	10.0 mm
f_y	400.0 MPa

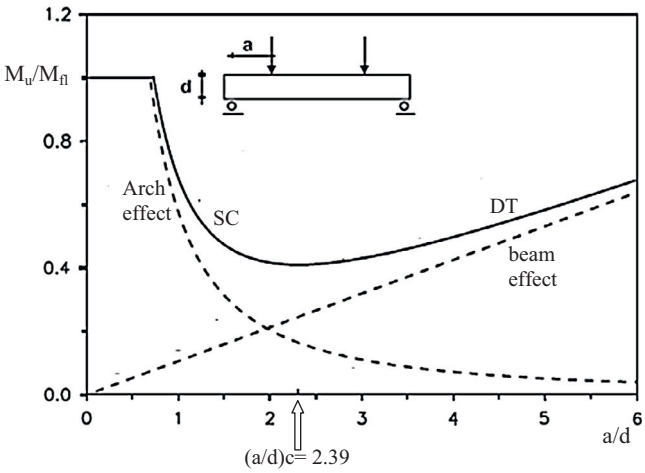

Figure 5 Failure effects of beams adopting Kani's Valley theory.

6. Position of strain gages

Strain gages were distributed along main reinforcement, and shear reinforcement. One strain gage was placed at each stirrup, while three strain gages were placed on main tension reinforcement at midspan and in the mid of shear spans. Another group of strain gages was placed at concrete surface, at midspan in compression side atop and front faces of the beam, and two other strain gages were placed at tension side in the path of shear cracks as shown in Fig. 6.

7. Stage two, plain concrete matrix

The second stage took place after testing the first pilot beam and determining the favorable crack site and direction for such beam geometry. Fig. 7 demonstrates that A typical shear crack failure was achieved for the cracks group positioned at the neutral axis of the beam at a distance of $L\backslash 5$ from the support with an angle of 45° regarding the axis of the specimen. For the second stage, two couples of beams with plain concrete matrix and SFRC matrix were manufactured. One beam was left virgin without any precracks to work as a control referenced beam while the other one was fabricated with one precrack at the favorable site and direction predicted from the pilot study only at one side and the other side left intact. The same dimensioning, caging, materials, and strain gage configurations of the pilot beam were adopted in the second stage.

8. Test results and discussion

The pilot RC beam described in stage one was examined to understand the shear failure behavior of RC beams and to distinct the site of shear crack initiation and its direction. Fig. 8

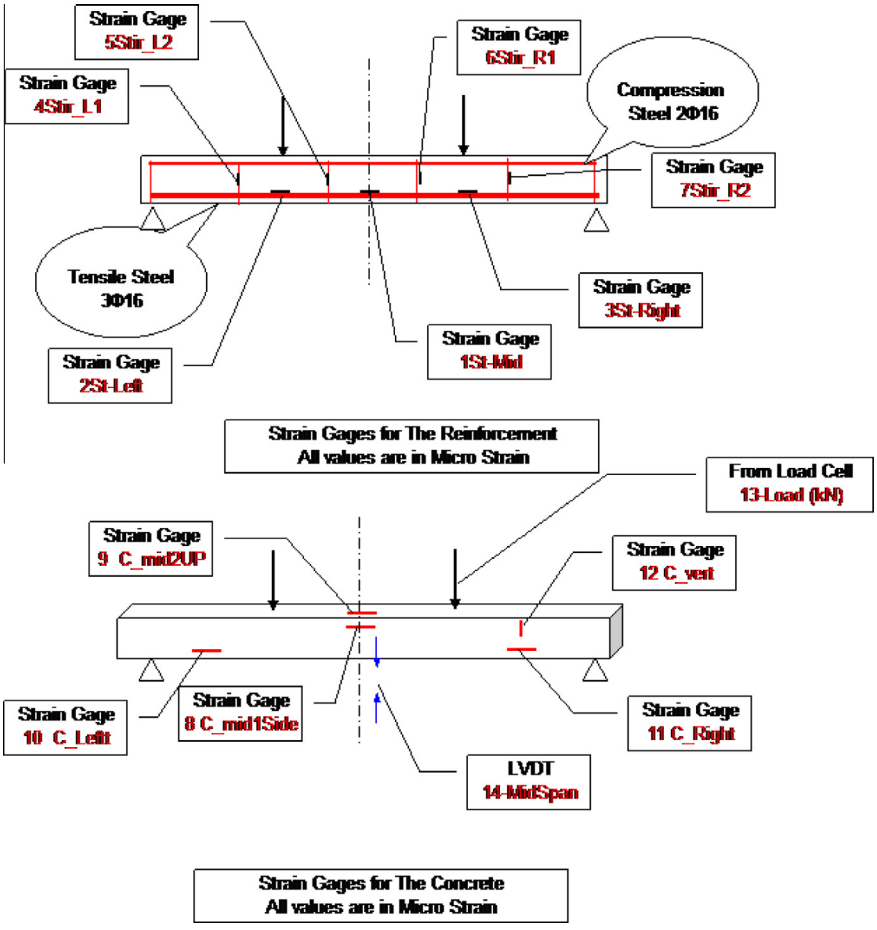

Figure 6 Positions of strain gages.

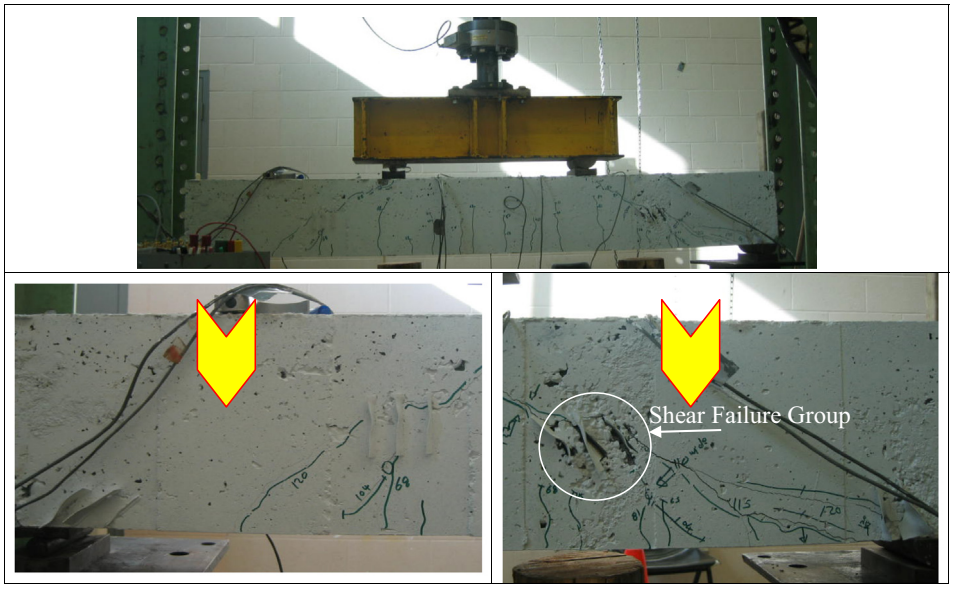

Figure 7 Shear failure group.

shows the crack patterns of this beam. After applying the stroke controlled four point bending loading regimen, the first flexural crack was observed at about 46 kN with long length at the tension side (bottom fiber of the beam) of the zero shear maximum moment domain as shown in Fig. 9. First shear cracks were observed at about 63 kN, due to the effect of

Figure 8 Crack patterns of RC beam with pre-cracks at different locations and orientations.

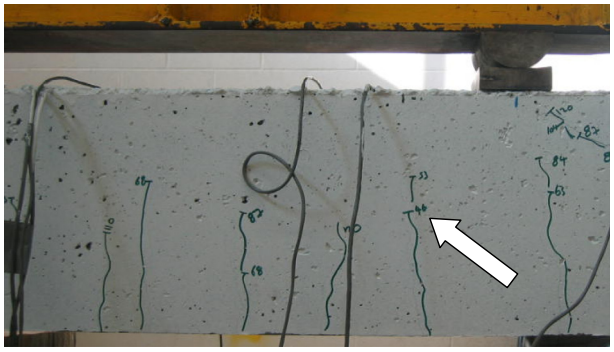

Figure 9 Crack patterns in zero shear.

constraint release at midheight of the beam and near supports in the vicinity of precrack groups. Shear cracks did not start from the tips of generated flexural cracks, instead, shear cracks started at the tips of pre-cracks. Two possible scenarios were expected, to have shear cracks at the tips of precrack groups inserted at maximum shear near the supports, which did not occur, or to have shear cracks growing from tips of precrack groups at midheight of the specimen in shear spans, which really happened leading to the scene. Shear cracks started in both shear spans at the lower tips of both types of pre-cracks at the mid-height of the beam (vertical, and diagonal groups) toward the tension side as shown in Fig. 10. At a load of about 80 kN the shear crack emanated from inclined pre-crack group grew rapidly from both sides (tension and compression) and became taller and wider leading to the failure mechanism until reaching the maximum failure load of 120 kN. On the other hand, stress relaxation was observed in the other shear span. Shear cracks at vertical pre-crack group did not grew any more as shown in Fig. 10. After reaching the maximum load of 120 kN the applied load relaxed with increased deflection

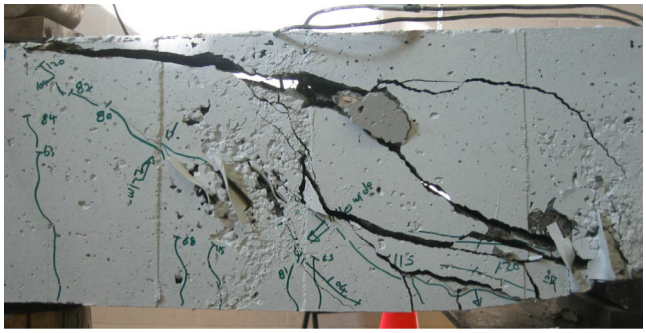

Figure 11 Arch failure mode after diagonal tension failure.

due to the loss of beam strength and by increasing the deflection the arch failure took place as shown in Fig. 11.

Fig. 12 shows the central deflection and the strains in tensile steel and stirrups in different locations against applied load. As predicted, the tensile strain at bottom steel in zero shear is higher than those in shear spans. The experimental results showed a little contribution of lower reinforcement to resist shear cracks as the tensile strain is similar in both shear spans in spite of the observed dominant crack in first shear span. Furthermore, the stirrup near the dominant shear crack suffered from a large tensile strain. The tensile strains in stirrups in zero shear and in shear span with narrow shear cracks are similar. This means that, one of the main objectives of stirrups is to connect the lower reinforcement to the upper one to maintain the integrity of the beam as previously examined by Sallam and Fawzy [11]. The strain in all stirrups was almost the same (value and increase rate) until reaching load of 63 kN then the rate of strain increased at both shear spans due to the formation of first shear cracks then at a load level of almost 80 kN a tremendous increased strain was observed at the first shear span where the leading shear crack took place at the inclined precrack group as shown in Fig. 12.

Data collected from strain gages placed at concrete surface were totally a miss, those gages at tension side in front of the cracks were damaged once the shear cracks propagate, while those on the midspan at the compression side gave distracting results leaving a big question mark on the feasibility of using strain gages on concrete surface!!.

For excessive deflection accompanied with arch failure mode, elevated strains at the stirrup controlling the failure accompanied with concrete crushing at upper surface of the beam in front of the shear crack made the stirrup to flatten

First Shear Span Second Shear Span

Figure 10 Crack patterns in shear spans.

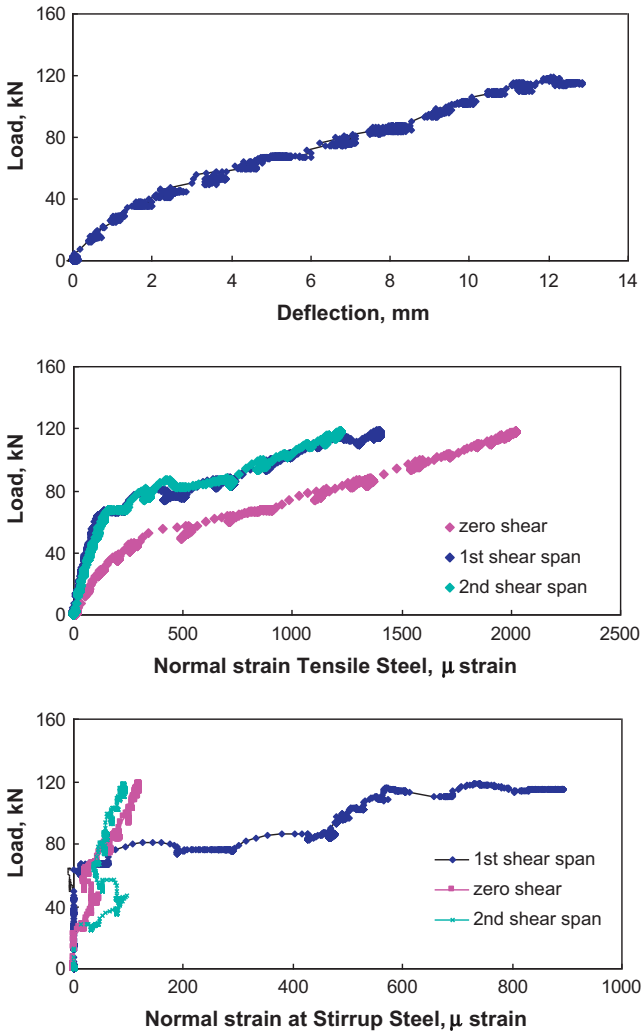

Figure 12 The central deflection and the strains in tensile steel and stirrups in different locations against applied load.

untying the clamped hocks at ends of the stirrup as shown in Fig. 13.

For the second stage of testing, a couple of beams with plain concrete matrix were tested. The beam with a single crack in the favorable position showed almost the same behavior of the pilot beam, while the control beam showed different behavior. The failure mechanism in the control beam was also due to

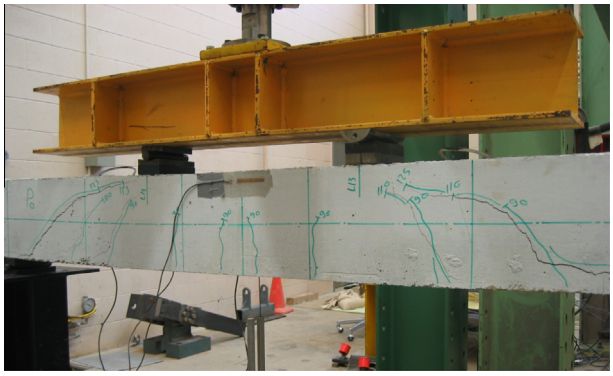

Figure 14 Diagonal tension failure at both sides of control beam.

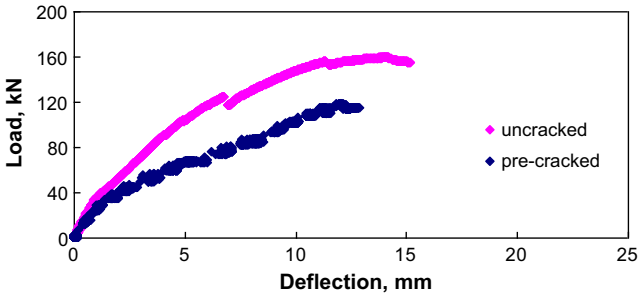

Figure 15 The effect of pre-crack on the stiffness and the capacity of RC beam.

diagonal tension but at both sides and at elevated level of load reaching 165 kN, and the first shear cracks were generated at the tips of flexural cracks as shown in Fig. 14.

The effect of pre-shear-crack on the stiffness and the capacity of RC beam is shown in Fig. 15. It is clear that, the presence of pre-crack reduced both the stiffness and the ultimate load of the beam.

Another couple of beams with short steel hooked fiber reinforced concrete matrix were tested. The beam with a single crack in the favorable position showed almost the same behavior of the virgin control beam. The effect of fiber bridging in front of the precrack eliminated the effect of constraint release in the favorable shear crack position, while the effect of artificial ductility increased markedly both the accompanied failure strain and the toughness of the beam.

Figure 13 Untied stirrup in arch failure mode.

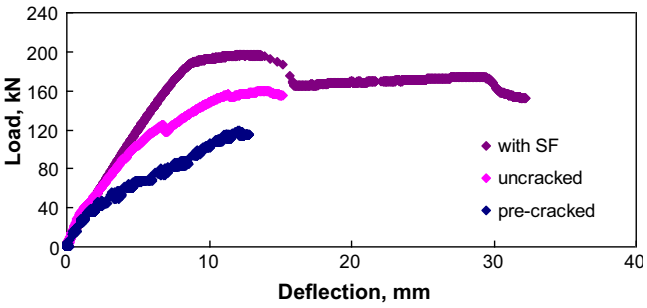

Figure 16 The effect of SF on the stiffness and the capacity of RC beam.

The effect of short steel hooked fiber on the stiffness and the capacity of RC beam is shown in Fig. 16. It is clear that, the presence of short steel hooked fiber increased both the stiffness and the ultimate load of the beam.

9. Conclusions

Based on the experimental results obtained and within the scope of this study the following conclusions can be drawn:

1. As a result of constraint release the first diagonal tension crack initiated from the bottom tip, i.e. tension side, of the diagonal pre-crack at first shear span and at midheight of the beam.
2. The tensile strains in stirrups in zero shear and in shear span with narrow shear cracks are similar, proving that, one of the main objective of stirrups is to connect the lower reinforcement to the upper one to maintain the integrity of the beam.
3. In fiber reinforced concrete beam a couple of diagonal tension cracks initiated at both sides from the tip of flexural cracks regardless of the existence of a mid-height pre-crack at one side of the beam, due to the effect of fiber bridging.
4. The feasibility of using strain gages on concrete surface needs further investigations.

Acknowledgment

The effort and Support of late Professor Khalid Soudki, University of Waterloo, Canada, to produce this work was gratefully acknowledged.

References

[1] ACI Committee 318. Building Code Requirements for Structural Concrete (ACI 318-05) and Commentary (318R-05). Farmington Hills, Mich: American Concrete Institute; 2005. p. 430.
[2] AASHTO LRFD. Bridge design specifications and commentary. 3rd ed., Washington, D.C.: American Association of State Highway Transportation Officials; 2004. p. 1264.
[3] CEN. BS EN 1992-1-1:2004 Eurocode 2. Design of concrete structures. Part 1: General rules and rules for buildings; 2004. p. 230.
[4] CSA Committee A23.3. Design of concrete structures (CSA A23.3-04). Mississauga: Canadian Standards Association; 2004. p. 214.
[5] JSCE. Specification for design and construction of concrete structures: design. JSCE standard, Part 1. Tokyo: Japan Society of Civil Engineers; 1986.
[6] Bentz EC, Vecchio FJ, Collins MP. Simplified modified compression field theory for calculating shear strength of reinforced concrete elements. ACI Struct J 2006;103(4):614–24.
[7] Bazant ZP, Kim JK. Size effect in shear failure of longitudinally reinforced beams. ACI Struct J 1984;81(5):456–68.
[8] MacGregor JG, Bartlett FM. Reinforced concrete – mechanics and design. Scarborough, Canada: Prentice Hall Canada Inc.; 2000, p. 1041.
[9] Kani GNJ. Basic facts concerning shear failure, of ACI. J Proc 1966;63(6):675–92.
[10] Kani GNJ. The riddle of shear failure and its solution. J ACI 1964;61(April):441–67.
[11] Sallam HEM, Fawzy Kh. Stirrups in RC beams: facts beyond assumptions. 5th ICCAE Conf 23–25 November. Cairo, Egypt: The Military Technical College; 2004.

Dr. **Hesham Abou-ElMal** is an assistant Professor in the Civil Engineering Department, Menofia University, Shibin El-Kom, Egypt. His research interests are Failure Analysis, Fracture Mechanics, Fiber Reinforced Concrete, and Strengthening of Structures. E-mail: heshnan@yahoo.com.

Dr. **Amr Sherbini** is an assistant Professor in the Civil Engineering Department, Suez Canal University, Ismailia, Egypt. His research interests are Fracture Mechanics, Fiber Reinforced Concrete, and Strengthening of Structures. E-mail: amrsukr@yahoo.com.

Prof. Dr. **Hossam Sallam** is a Professor in the Materials Engineering Department, Zagazig University, Zagazig, Egypt. His research interests are Fracture Mechanics, Fiber Reinforced Concrete, and Strengthening of Structures. E-mail: hem_sallam@yahoo.com.